



Integrated FY-2021 Elevated-Temperature Mechanical-Testing Results for Alloy 709 Code Case

September 2021

Ryann Rupp
Idaho National Laboratory

Yanli Wang
Oak Ridge National Laboratory

Xuan Zhang
Argonne National Laboratory

Ting-Leung Sham
Idaho National Laboratory



DISCLAIMER

This information was prepared as an account of work sponsored by an agency of the U.S. Government. Neither the U.S. Government nor any agency thereof, nor any of their employees, makes any warranty, expressed or implied, or assumes any legal liability or responsibility for the accuracy, completeness, or usefulness, of any information, apparatus, product, or process disclosed, or represents that its use would not infringe privately owned rights. References herein to any specific commercial product, process, or service by trade name, trade mark, manufacturer, or otherwise, does not necessarily constitute or imply its endorsement, recommendation, or favoring by the U.S. Government or any agency thereof. The views and opinions of authors expressed herein do not necessarily state or reflect those of the U.S. Government or any agency thereof.

Integrated FY-2021 Elevated-Temperature Mechanical- Testing Results for Alloy 709 Code Case

Ryann Rupp
Idaho National Laboratory

Yanli Wang
Oak Ridge National Laboratory

Xuan Zhang
Argonne National Laboratory

Ting-Leung Sham
Idaho National Laboratory

September 2021

**Idaho National Laboratory
Advanced Reactor Technologies
Idaho Falls, Idaho 83415**

<http://www.art.inl.gov>

**Prepared for the
U.S. Department of Energy
Office of Nuclear Energy
Under DOE Idaho Operations Office
Contract DE-AC07-05ID14517**

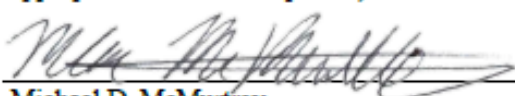
Page intentionally left blank

INL ART Program

**Integrated FY-2021 Elevated-Temperature
Mechanical-Testing Results for Alloy 709 Code Case**

INL/EXT-21-64314
Revision 0
September 2021

Technical Reviewer: (Confirmation of mathematical accuracy, and correctness of data and appropriateness of assumptions.)



Michael D. McMurtrey

9/9/2021
Date

Approved by:

M. Davenport

Michael E. Davenport
ART Project Manager

9/9/2021
Date

Travis Mitchell

Travis R. Mitchell
ART Program Manager

9/9/2021
Date

Michelle Sharp

Michelle T. Sharp
INL Quality Assurance

9/9/2021
Date

Page intentionally left blank

SUMMARY

This report provides the status of creep, fatigue, and creep-fatigue testing that transpired in fiscal year (FY)-2021 at Argonne National Laboratory (ANL), Idaho National Laboratory (INL), and Oak Ridge National Laboratory (ORNL). This testing is being conducted to develop the data package to qualify Alloy 709 in Section III, Division 5 of the American Society of Mechanical Engineers (ASME) Boiler and Pressure Vessel Code (BPVC). This would permit the use of Alloy 709 for elevated-temperature nuclear construction. Preliminary results continue to demonstrate the improved creep and fatigue resistance of Alloy 709 compared to 316H stainless steel.

ACKNOWLEDGEMENTS

This research was sponsored by the United States (U.S.) Department of Energy (DOE) under Contract No. DE-AC07-05ID14517 with Idaho National Laboratory (INL), which is managed and operated by Battelle Energy Alliance; under Contract No. DE-AC05-00OR22725 with Oak Ridge National Laboratory (ORNL), which is managed and operated by the University of Tennessee–Battelle LLC; and under Contract No. DE-AC02-06CH11357 with Argonne National Laboratory (ANL), which is managed and operated by the University of Chicago–Argonne LLC. Programmatic direction was provided by the Office of Nuclear Reactor Deployment of the DOE Office of Nuclear Energy.

The authors gratefully acknowledge the support provided by Sue Lesica, Federal Lead for Advanced Materials, Advanced Reactor Technologies (ART) Program; Brian Robinson, Federal Manager, ART Fast Reactors (FR) Campaign; and Robert Hill, ANL, National Technical Director, ART FR Campaign.

The authors are also grateful to Peijun Hou, who is affiliated with Imtech Corporation in Knoxville, TN, for creating the fatigue design curves and creep-fatigue interaction diagram. The authors also acknowledge helpful discussions with Richard Wright and Michael McMurtrey of INL and Meimei Li of ANL. Finally, the authors thank their support staff: C. Austin, ORNL; C.S. Hawkins, ORNL; K. Hedrick, ORNL; J.W. Jones, INL; E. Listwan, ANL; R.L. Rink, ANL; and J.A. Simpson, INL, for their technical support.

CONTENTS

SUMMARY	v
ACKNOWLEDGEMENTS.....	vi
ACRONYMS.....	ix
1. MOTIVATION	1
2. BACKGROUND.....	2
2.1 Alloy 709.....	2
2.2 Larson-Miller Parametric Correlation.....	3
2.3 Creep-fatigue Interaction Diagram	3
3. MATERIAL	6
4. CREEP CODE CASE TESTING.....	7
4.1 FY-2021 Progress	7
4.2 Results.....	10
5. FATIGUE CODE CASE TESTING	14
5.1 FY-2021 Progress	14
5.2 Results.....	14
6. CREEP-FATIGUE CODE CASE TESTING	17
6.1 FY-2021 Progress	17
6.2 Results.....	17
7. SUMMARY AND ONGOING WORK.....	19
8. REFERENCES.....	20

FIGURES

Figure 1. Rupture-stress ratio of ESR1150AH and NF709 compared to 316H SS as a function of temperature for: (a) a 100,000-hour lifetime; and (b) a 300,000-hour lifetime.	11
Figure 2. Optimized Larson-Miller correlation for: (a) ESR1150AH; (b) NF709; and (c) 316H SS.	12
Figure 3. Preliminary fatigue design curve of Alloy 709 at 649°C (1200°F).	15
Figure 4. Preliminary fatigue design curve of Alloy 709 at 816°C (1500°F).	15
Figure 5. Preliminary creep-fatigue D-diagram for Alloy 709.	18

TABLES

Table 1. Chemistry composition, in weight percent, of the AOD1100, ESR1100, and ESR1150 plates as well the chemistry requirements specified in ASME SA-213 for UNS S31025 (ASME, 2021c).....	6
Table 2. Summary of creep-rupture testing during FY-2021.....	8
Table 3. Creep-rupture tests of the AOD1100 processing condition that transpired during FY-2021.....	8
Table 4. Creep-rupture tests of the ESR1100 processing condition that transpired during FY-2021.....	8
Table 5. Creep-rupture tests of the ESR1150AH processing condition that transpired during FY-2021.....	9
Table 6. Fatigue tests of the ESR1150AH processing condition that transpired during FY-2021.	14
Table 7. Creep-fatigue tests of the ESR1150AH processing condition that transpired during FY-2021.....	17

ACRONYMS

ANL	Argonne National Laboratory
AOD	argon oxygen decarburization
ART	Advanced Reactor Technologies
ASME	American Society of Mechanical Engineers
ASTM	American Society for Testing and Materials
ATI	Allegheny Technologies Incorporated
BPVC	Boiler and Pressure Vessel Code
DOE	U.S. Department of Energy
ESR	electroslag remelting
FR	Fast Reactors
FY	fiscal year
INL	Idaho National Laboratory
LMP	Larson-Miller parameter
NRC	U.S. Nuclear Regulatory Commission
ORNL	Oak Ridge National Laboratory
SFR	sodium-cooled fast reactor
SS	stainless steel
U.S.	United States

Page intentionally left blank

Integrated FY-2021 Elevated-Temperature Mechanical-Testing Results for Alloy 709 Code Case

1. MOTIVATION

President Biden’s Executive Order 14008 issued a federal directive for the development of a plan to facilitate a carbon-zero electric-industry sector by 2035 (Exec. Order No. 14008, 2021). Nuclear energy is one potential resource to satisfy this executive order. One of the leading advanced nuclear reactor concepts is the sodium-cooled fast reactor (SFR). Other needs not associated with this executive order, but important for clean energy—such as the recycling of spent nuclear fuel—can also be attained with SFRs (Sham and Natesan, 2017).

SFR commercialization is dependent upon these reactors being economically viable. A crucial aspect to achieving this commercialization is advanced materials, which can reduce capital constructions costs. Although advanced materials are typically more expensive than traditional steels, they offer advantages that may ultimately lead to savings. Advanced materials may enable higher operating temperatures, which improves thermal efficiency and leads to increased power output. Additionally, advanced materials may offer longer design lifetimes, meaning components may not have to be replaced as regularly. Besides economic savings, advanced materials may offer improved safety margins, material reliability, and design flexibility (Sham and Natesan, 2017).

Alloy 709, an austenitic stainless steel (SS), has been identified as an advanced material that would improve the viability of SFRs. Alloy 709 has better creep properties than 316H SS, the reference construction material for SFRs, but is not as expensive as nickel-based alloys usually used at high temperatures. This enables the construction of thinner walled components, reducing construction costs. Alloy 709 has an improved resistance to thermal gradients compared to 316H SS. This eliminates the need for expensive add-on hardware required for construction with 316H SS, further reducing construction costs. There are additional benefits beyond the two examples provided for constructing components with Alloy 709 as compared to 316H SS. Potential SFR components to be constructed with Alloy 709 are the reactor vessel, piping, core supports, intermediate heat exchanger, and compact heat exchanger. The compact heat exchanger could link the SFR to a supercritical carbon dioxide Brayton energy conversion system as one possible application (Sham and Natesan, 2017).

In the United States (U.S.), the U.S. Nuclear Regulatory Commission (NRC) licenses and regulates nuclear reactors and nuclear reactor designs. Nuclear plant owners and operators can take advantage of Section III, Division 5 of the American Society of Mechanical Engineers (ASME) Boiler and Pressure Vessel Code (BPVC) to reduce the effort needed to license a nuclear reactor or nuclear reactor design. This section of the Code provides design rules for elevated-temperature nuclear construction (ASME, 2021b). The NRC is in the process of evaluating the 2017 version of Section III, Division 5 for potential endorsement (Thomas, 2018). Alloy 709 is currently not qualified in Section III, Division 5 of the ASME BPVC. A program comprised of a collaboration between three U.S. Department of Energy (DOE) national laboratories—Argonne National Laboratory (ANL), Idaho National Laboratory (INL), and Oak Ridge National Laboratory (ORNL)—is in progress to qualify Alloy 709 in Section III, Division 5 of the ASME BPVC through multiple Code Cases. These Code Cases require putting together data packages that involve conducting tests to collect Alloy 709 data from which the design rules will be established. The purpose of this report is to provide an update on the Alloy 709 Code Case regarding the status of testing as well as preliminary results. Focus will be on creep, fatigue, and creep-fatigue testing conducted at ANL, INL, and ORNL. To date, Code Case testing has been conducted on the Electralloy/G.O. Carlson A709 commercial heat. Emphasis in this report will be placed on work performed in fiscal year (FY)-2021.

2. BACKGROUND

2.1 Alloy 709

Alloy 709 is an austenitic SS that originated from NF709, which was developed as a tubing material for ultra-supercritical boiler applications by Nippon Steel. NF709 is strengthened by molybdenum and nitrogen in solution as well as carbonitride precipitates. NF709 was designed so that detrimental intermetallics do not precipitate during long-term, elevated-temperature service (Sham and Natesan, 2017). NF709 is included in American Society for Testing and Materials (ASTM) specification A213 and ASME specification SA-213. Both specifications are entitled “Standard Specification for Seamless Ferritic and Austenitic Alloy-Steel Boiler, Superheater, and Heat Exchanger Tubes.” NF709 is designated as grade TP310MoCbN and UNS S31025 (ASTM, 2021; ASME, 2021c). ASME BPVC Case 2581 qualifies Section I construction of NF709 seamless tubes for temperatures up to 815°C (1500°F) (ASME, 2021e).

A collaboration between ANL, INL, and ORNL was initiated in 2013 to develop Alloy 709 plate and characterize its properties. This work resulted in the recommendation to qualify Alloy 709 in Section III, Division 5 of the ASME BPVC for elevated-temperature nuclear construction. This recommendation was based on the following findings: (1) Alloy 709 is stable in an elevated-temperature, liquid-sodium environment; (2) Alloy 709 can be successfully welded with Alloy 625 or optimized Alloy 709 filler metals by automated gas-tungsten arc welding; (3) the production of Alloy 709 can be optimized to improve the creep-fatigue properties while maintaining creep strength; and (4) the properties of Alloy 709 are improved compared to 316H SS, which is qualified in Section III, Division 5 of the ASME BPVC (Sham and Natesan, 2017).

A plan for developing the data package needed to qualify Alloy 709 in Section III, Division 5 of the ASME BPVC was formulated. Multiple data packages were devised through a staged qualification approach for Alloy 709 to support multiple code cases with increasing design lives. This approach entails qualifying a material for a shorter design life initially using data that can be generated in the near term. The qualified design life is extended at a later date once the longer-term data needed to support this extension, such as creep and thermal aging, becomes available. This enables accelerated qualification of Alloy 709. The alternative, non-accelerated approach, is to wait until all necessary data to support a Code Case for the longest design life is generated. This plan took into consideration the needs of both the ASME BPVC and NRC (Sham and Natesan, 2017). This includes Nonmandatory Appendix HBB-Y in Section III, Division 5 of the ASME BPVC, which provides guidelines for qualifying new materials, as well as re-occurring issues flagged by the NRC (Sham and Natesan, 2017; ASME, 2021b; O'Donnell and Griffin, 2007). Nonmandatory Appendix HBB-Y specifies that the data package for qualifying new materials must be comprised of data from a minimum of three heats, which need to encompass the composition range, product forms, and size of the components to be used in service (ASME, 2021b).

The first commercial heat of Alloy 709 was procured in FY-2017 from Electralloy/G.O. Carlson, heat 58776. This heat was procured in a manner that enabled the final processing step and the solution annealing temperature to be independently investigated. The final processing step was either argon oxygen decarburization (AOD), electroslag remelting (ESR), or ESR with a homogenization treatment (ESR + HOMO). The plates were solution annealed at 1050°C (1922°F), 1100°C (2012°F), or 1150°C (2102°F). A total of nine unique groups of plates were fabricated, one for each processing combination (Natesan et al., 2017). Creep, fatigue, and creep-fatigue testing were initiated to down-select the final processing step and solution anneal temperature. Plates that were solution annealed at 1050°C (1922°F) were eliminated from consideration because of a too fine grain size and an unacceptably short creep-rupture lifetime. The ESR final processing condition resulted in longer elongations to failure during creep, establishing it as the best method of manufacturing. A tradeoff between creep and creep-fatigue properties was found between the solution annealing temperatures. The plate with the ESR final processing step,

solution annealed at 1150°C (2102°F) had the best creep-rupture properties but inadequate creep-fatigue properties. For the remainder of this report, this processing condition will be referred to as ESR1150. The processing condition that resulted in the optimal balance in properties was the ESR plate solution annealed at 1100°C (2012°F), although the creep-fatigue properties were worse than desired (McMurtrey, 2018; McMurtrey and Rupp, 2019; Natesan, Zhang, and Li, 2018; Wang et al., 2018). For the remainder of this report, this condition will be labeled ESR1100. During this time, preliminary results prompted ORNL to start long-term tests of Alloy 709 fabricated with AOD and solution annealed at 1100°C (2012°F) (Wang et al., 2018; Wang and Sham, 2019; Wang, Hou, and Sham, 2020; Wang, Hou, and Sham, 2021). For the remainder of this report, this processing combination will be referred to as AOD1100. Later findings resulted in ESR1100 tests being started at ANL and ORNL (Wang and Sham, 2019; Wang, Hou, and Sham, 2020; Wang, Hou, and Sham, 2021; Zhang and Sham, 2019; Zhang and Sham, 2020).

A heat treatment to age-harden Alloy 709 was developed in FY-2019. This heat treatment emanated from two questions. The first was concerning whether the beneficial precipitates that form during accelerated testing would form during service at low temperature, low stress conditions. The second was whether the Alloy 709 properties, particularly the creep-fatigue properties, could be further improved. Heat treating Alloy 709 prior to service would ensure that the beneficial precipitates would be present during service conditions. The heat treatment needed to precipitate the beneficial MX (Nb, Ti, V: C, N) and Z-phase (CrNbN) without forming the detrimental intermetallics (Fe₂Mo, Fe₂Nb). A 10-hour, 775°C (1427°F) heat treatment protocol was identified (Zhang, Sham, and Young, 2019). This heat treatment promoted the precipitation of the beneficial MX and Z-phase and was observed to improve creep-fatigue properties without significantly impacting creep properties (Rupp and McMurtrey, 2020). ESR1150 subsequently heat treated at 775°C (1427°F) for 10 hours has been identified as having the best properties. For the remainder of this report, this Alloy 709 condition will be referred to as ESR1150AH. Testing of the ESR1150AH material to develop the data package to qualify Alloy 709 in Section III, Division 5 of the ASME BPVC is in progress (Wang, Hou, and Sham, 2021; Zhang, Sham, and Li, 2021).

2.2 Larson-Miller Parametric Correlation

The Larson-Miller parametric correlation enables creep-rupture behavior to be correlated with stress. Temperature and time are combined into a single parameter identified as the Larson-Miller parameter (LMP). The LMP is defined in Equation (1) as:

$$\text{LMP} = (T + 273.15) (C + \log(t_r)) = a_0 + a_1 \log(S) + a_2 (\log(S))^2 + a_3 (\log(S))^3 + \dots \quad (1)$$

where:

T = temperature, °C

C = material-dependent constant

t_r = rupture time, hr.

a_i = constants that are impacted by the number of polynomial terms to fit the rupture data

S = stress, MPa

log = logarithm in base 10 (Larson and Miller, 1952; Swindeman et al., 2007).

2.3 Creep-fatigue Interaction Diagram

Section III, Division 5 of the ASME BPVC (ASME, 2021b) uses the creep-fatigue interaction diagram, also known as the D-diagram, to evaluate creep-fatigue life. This approach evaluates the creep and cyclic damage separately and considers the interaction through the D-diagram using the following equations:

$$D_f = \sum_j \left(\frac{n}{N_d} \right)_j \quad (2)$$

$$D_c = \sum_k \left(\frac{\Delta t}{T_d} \right)_k \quad (3)$$

$$D_f + D_c \leq D \quad (4)$$

where:

D_f = cyclic (fatigue) damage fraction

n = the number of cycles of type j

N_d = the allowable number of cycles of the same type as n

D_c = creep damage fraction

Δt = time at stress level k

T_d = allowable time at stress level k

D = the allowable damage fraction for the combined creep and cyclic damage.

Figure HBB-T-1420-2 in Section III, Division 5 of the ASME BPVC (ASME, 2021b) is the D-diagram for the various qualified alloys. The x- and y-axes are D_f and D_c , respectively. The bilinear curves form the damage envelope for each alloy and bounds the design limits for the calculated damage (Wright et al., 2016). The D-diagram provides the nominal behavior of the creep and cyclic interaction. Designs that fall to the left of the bilinear curves are considered acceptable. The D-diagram is developed using standard creep-fatigue test results at various test temperatures, hold times, and strain rates. A description for calculating D_f and D_c for each individual creep-fatigue test is provided in the following paragraphs.

D_f is calculated by dividing the number of creep-fatigue cycles to failure by the number of fatigue cycles to failure. Consequently, this calculation requires at least one fatigue test from the same product form with the same test conditions as the creep-fatigue test. If multiple fatigue tests meet these requirements, the average number of cycles to failure for all applicable fatigue tests is used (Wright et al., 2016).

D_c is defined as the total creep damage accumulated during the tensile hold for each cycle until failure. This calculation can be simplified by approximating D_c as:

$$D_c = N_f \times D_{c, \text{midlife}} \quad (5)$$

where:

N_f = number of cycles to failure

$D_{c, \text{midlife}}$ = creep damage fraction calculated at the midlife cycle.

The stress-relaxation curve and Equation (6) are used to calculate $D_{c, \text{midlife}}$:

$$D_{c, \text{midlife}} = \int_{t_0}^{t_h} \left(\frac{1}{T_d} \right) dt \quad (6)$$

where:

t_0 = time at the beginning of the tensile hold

t_h = time at the end of the tensile hold.

The Larson-Miller parametric correlation, Equation (1), can be used to determine T_d . This correlation should be established from the same heat of material as the creep-fatigue specimen. In practice, the nominal LMP correlation for all available heats is used. If $a_i = 0$ in Equation (1) for $i \geq 2$, then the allowable time can be expressed as:

$$T_d = 10^{(-C + \frac{a_0}{(T+273.15)})} \times \sigma^{\left(\frac{a_1}{(T+273.15)}\right)} \quad (7)$$

with the units of hours (Wright et al., 2016). Integration of $\frac{1}{T_d}$ can be achieved using Riemann sums or fitting a power-law trend curve to the stress-relaxation data (Wright et al., 2016).

3. MATERIAL

Alloy 709, heat 58776, was procured from Electralloy/G.O. Carlson in the solution annealed condition. In FY-2021, three different processing conditions were investigated: AOD1100, ESR1100, and ESR1150AH. The chemical composition of the AOD1100, ESR1100, and ESR1150 plates are shown in Table 1. The chemistry requirements specified in SA-213 for UNS S31025 are also provided in Table 1 for comparison (ASME, 2021c). The AOD plate is 1.2 in. thick, while the ESR plates are 1.1 in. thick. The microstructure, grain size, hardness, and tensile properties of these plates are available in a 2017 report (Natesan et al., 2017). The ESR1150 material was heat treated at 775°C (1427°F) for 10 hours and subsequently air cooled in order to age harden the material to the ESR1150AH condition.

Table 1. Chemistry composition, in weight percent, of the AOD1100, ESR1100, and ESR1150 plates as well the chemistry requirements specified in ASME SA-213 for UNS S31025 (ASME, 2021c).

	C	Mn	Si	P	S	Cr	Ni	Mo
AOD1100	0.07	0.91	0.44	0.014	< 0.000	19.93	24.98	1.51
ESR1100/ ESR1150	0.066	0.90	0.38	0.014	0.001	20.05	25.14	1.51
UNS S31025	0.10 max	1.50 max	1.00 max	0.030 max	0.030 max	19.5 – 23.0	23.0 – 26.0	1.0 – 2.0

	N	Nb	Ti	Cu	Co	Al	B	Fe
AOD1100	0.148	0.26	0.04	0.06	0.02	0.02	0.0045	Bal.
ESR1100/ ESR1150	0.152	0.26	0.01	0.06	0.02	0.02	0.0030	Bal.
ASME SA-213	0.10 – 0.25	0.10 – 0.40	0.20 max	–	–	–	0.002 – 0.010	–

Bal. = Balance

4. CREEP CODE CASE TESTING

4.1 FY-2021 Progress

In FY-2021, a total of 24 creep-rupture tests were completed. Another 53 creep-rupture tests are currently in progress at the time of writing this report. These tests were conducted at ANL, INL, and ORNL for the AOD1100, ESR1100, and ESR1150AH processing conditions. These tests can be further divided by its purpose. The four categories are preliminary, 100,000-hour, 300,000-hour, and 500,000-hour, which indicates the Code Case that the test aims to support. The maximum estimated rupture life for each of these categories is 11,000 hours, 25,000 hours, 68,000 hours, and 110,000 hours, respectively. A breakdown of these tests by processing condition, category, and laboratory are summarized in Table 2. The test conditions for each of these tests are described in Table 3, Table 4, and Table 5 for the AOD1100, ESR1100, and ESR1150AH processing conditions, respectively. The five tests in Table 5 with the status labeled as ‘queue’ are the next tests that are planned. At minimum, two of these tests will be started in FY-2021. The other three tests will be started as creep frames become available.

Creep-rupture tests were conducted in accordance with ASTM E139 (ASTM, 2011). Tests conducted at INL are also in accordance with PLN-3386 (Idaho National Laboratory, 2016). Cylindrical test specimens were used with the longitudinal direction parallel to the rolling direction of the plate. Specimens were machined from the center of the plate with respect to the plate thickness, per ASTM guidance. Specimens tested at ANL and INL had a 6.35 mm (0.250 in.) minimum diameter and a reduced parallel section that was at minimum 31.75 mm (1.250 in.). A modified test specimen geometry was used at ORNL with a 9.53 mm (0.375 in.) gauge diameter and a nominal gauge length of 47.63 mm (1.875 in.). This gauge diameter is larger than the conventional 6.35 mm diameter creep specimen in order to reduce the effect of oxidation. This is necessary to support very long-term testing. Increasing the diameter of the specimen decreases the surface-to-volume ratio, which consequently decreases the effect of oxidation. For consistency, this specimen geometry is also used for short-term and intermediate-term testing. Test conditions were selected to generate creep-rupture data to cover a wide range of LMPs. These conditions also took Section III, Division 5, Nonmandatory Appendix HBB-Y and Section II, Part D, Mandatory Appendix 5 into consideration (ASME, 2021b; 2021a). As tests finish and new data becomes available, the growing data package is continuously evaluated for gaps, and if identified, requisite tests are added to the test plan.

Table 2. Summary of creep-rupture testing during FY-2021.

Processing Condition	Category	Laboratory	Number of Tests Completed in FY-2021	Number of Tests in Progress at the Time of Writing this Report
AOD1100	100,000/300,000/500,000 hours	ORNL	2	4
ESR1100	100,000 hours	ANL	1	0
	300,000/500,000 hours	ORNL	0	12
ESR1150AH	Preliminary	ANL	10	9
		INL	5	3
		ORNL	6	10
	100,000 hours	ANL	0	4
		INL	0	3
		ORNL	0	2
	300,000 hours	ORNL	0	3
	500,000 hours	ORNL	0	3

Table 3. Creep-rupture tests of the AOD1100 processing condition that transpired during FY-2021.

Temperature	Stress	Responsible Lab	Status	Sample ID
300,000/500,000 hour				
550°C (1022°F)	309 MPa (44.8 ksi)	ORNL	In progress	TN33629
600°C (1112°F)	204 MPa (29.6 ksi)	ORNL	Complete	TN33630
650°C (1202°F)	134 MPa (19.1 ksi)	ORNL	Complete	TN33631
700°C (1292°F)	88 MPa (12.8 ksi)	ORNL	In progress	TN33632
750°C (1382°F)	58 MPa (8.4 ksi)	ORNL	In progress	TN33636
800°C (1472°F)	38 MPa (5.5 ksi)	ORNL	In progress	TN33635

Table 4. Creep-rupture tests of the ESR1100 processing condition that transpired during FY-2021.

Temperature	Stress	Responsible Lab	Status	Sample ID
100,000 hour				
550°C (1022°F)	355 MPa (51.5 ksi)	ANL	Complete	BB2-15
300,000/500,000 hour				
525°C (977°F)	355 MPa (51.5 ksi)	ORNL	In progress	TN34162
550°C (1022°F)	330 MPa (47.9 ksi)	ORNL	In progress	TN34163
550°C (1022°F)	285 MPa (41.3 ksi)	ORNL	In progress	TN34182
575°C (1067°F)	285 MPa (41.3 ksi)	ORNL	In progress	TN34183
600°C (1112°F)	200 MPa (29.0 ksi)	ORNL	In progress	TN34130
625°C (1157°F)	155 MPa (22.5 ksi)	ORNL	In progress	TN34113
700°C (1292°F)	90 MPa (13.0 ksi)	ORNL	In progress	TN34111
700°C (1292°F)	80 MPa (11.6 ksi)	ORNL	In progress	TN34161
725°C (1337°F)	80 MPa (11.6 ksi)	ORNL	In progress	TN34112
750°C (1382°F)	60 MPa (8.7 ksi)	ORNL	In progress	TN34184
800°C (1472°F)	40 MPa (5.8 ksi)	ORNL	In progress	TN34241
800°C (1472°F)	35 MPa (5.1 ksi)	ORNL	In progress	TN34265

Table 5. Creep-rupture tests of the ESR1150AH processing condition that transpired during FY-2021.

Temperature	Stress	Responsible Lab	Status	Sample ID
Preliminary				
600°C (1112°F)	250 MPa (36.3 ksi)	ANL	In progress	A709-ESR1150AH-13
625°C (1157°F)	250 MPa (36.3 ksi)	ANL	Complete	A709-ESR1150AH-7
650°C (1202°F)	250 MPa (36.3 ksi)	ANL	Complete	A709-ESR1150AH-1
625°C (1157°F)	200 MPa (29.0 ksi)	ANL	In progress	A709-ESR1150AH-14
650°C (1202°F)	200 MPa (29.0 ksi)	ANL	Complete	A709-ESR1150AH-6
650°C (1202°F)	175 MPa (25.4 ksi)	ANL	Complete	A709-ESR1150AH-10
675°C (1247°F)	175 MPa (25.4 ksi)	ANL	Complete	A709-ESR1150AH-4
650°C (1202°F)	155 MPa (22.5 ksi)	INL	Complete	BCHT-IC-6
675°C (1247°F)	150 MPa (21.8 ksi)	ANL	In progress	A709-ESR1150AH-20
700°C (1292°F)	150 MPa (21.8 ksi)	ANL	In progress	A709-BC2-AH-01
675°C (1247°F)	140 MPa (20.3 ksi)	ANL	In progress	A709-ESR1150AH-11
700°C (1292°F)	140 MPa (20.3 ksi)	ANL	Complete	A709-ESR1150AH-5
725°C (1337°F)	140 MPa (20.3 ksi)	ANL	Complete	A709-ESR1150AH-2
700°C (1292°F)	110 MPa (16.0 ksi)	ANL	In progress	A709-ESR1150AH-12
725°C (1337°F)	110 MPa (16.0 ksi)	ANL	Complete	A709-ESR1150AH-8
750°C (1382°F)	110 MPa (16.0 ksi)	ANL	Complete	A709-ESR1150AH-3
725°C (1337°F)	82 MPa (11.9 ksi)	ANL	In progress	A709-ESR1150AH-15
750°C (1382°F)	82 MPa (11.9 ksi)	INL	Complete	BCHT-IC-8
775°C (1427°F)	82 MPa (11.9 ksi)	ANL	Complete	A709-ESR1150AH-9
750°C (1382°F)	75 MPa (10.9 ksi)	ANL	In progress	A709-BC2-AH-02
775°C (1427°F)	75 MPa (10.9 ksi)	ANL	In progress	A709-BC2-AH-03
750°C (1382°F)	65 MPa (9.4 ksi)	INL	In progress	BCHT2-IC-02
775°C (1427°F)	65 MPa (9.4 ksi)	INL	Queue	
800°C (1472°F)	65 MPa (9.4 ksi)	INL	Complete	BCHT-IC-12
800°C (1472°F)	45 MPa (6.5 ksi)	INL	Queue	
825°C (1517°F)	45 MPa (6.5 ksi)	INL	Queue	
850°C (1562°F)	45 MPa (6.5 ksi)	INL	In progress	BCHT2-IC-03
825°C (1517°F)	35 MPa (5.1 ksi)	INL	Queue	
850°C (1562°F)	35 MPa (5.1 ksi)	INL	Complete	BCHT-IC-7
875°C (1607°F)	35 MPa (5.1 ksi)	INL	Complete	BCHT-IC-11
850°C (1562°F)	30 MPa (4.4 ksi)	ORNL	In progress	TN39517
875°C (1607°F)	30 MPa (4.4 ksi)	ORNL	In progress	TN39518
900°C (1652°F)	30 MPa (4.4 ksi)	ORNL	Complete	TN39519
875°C (1607°F)	24 MPa (3.5 ksi)	ORNL	In progress	TN39694
900°C (1652°F)	24 MPa (3.5 ksi)	ORNL	Complete	TN39513
925°C (1697°F)	24 MPa (3.5 ksi)	ORNL	Complete	TN39501
900°C (1652°F)	20 MPa (2.9 ksi)	ORNL	In progress	TN39693
925°C (1697°F)	20 MPa (2.9 ksi)	ORNL	Complete	TN39511
950°C (1742°F)	20 MPa (2.9 ksi)	ORNL	Complete	TN39612
925°C (1697°F)	15 MPa (2.2 ksi)	ORNL	In progress	TN39842
950°C (1742°F)	15 MPa (2.2 ksi)	ORNL	In progress	TN39692
975°C (1787°F)	15 MPa (2.2 ksi)	ORNL	Complete	TN39512
975°C (1787°F)	15 MPa (2.2 ksi)	ORNL	In progress	TN39910
975°C (1787°F)	11 MPa (1.6 ksi)	ORNL	In progress	TN39843
1,000°C (1832°F)	10 MPa (1.5 ksi)	ORNL	In progress	TN40008
1,000°C (1832°F)	9 MPa (1.3 ksi)	INL	In progress	BCHT-IC-04

Temperature	Stress	Responsible Lab	Status	Sample ID
Preliminary (cont.)				
1,000°C (1832°F)	8 MPa (1.2 ksi)	INL	Queue	
1,000°C (1832°F)	7 MPa (1.0 ksi)	ORNL	In progress	TN40007
100,000 hour				
575°C (1067°F)	250 MPa (36.3 ksi)	ANL	In progress	A709-ESR1150AH-19
600°C (1112°F)	200 MPa (29.0 ksi)	ANL	In progress	A709-ESR1150AH-18
625°C (1157°F)	175 MPa (25.4 ksi)	ANL	In progress	A709-ESR1150AH-17
650°C (1202°F)	140 MPa (20.3 ksi)	ANL	In progress	A709-ESR1150AH-16
675°C (1247°F)	110 MPa (16.0 ksi)	INL	In progress	BCHT-IC-10
700°C (1292°F)	90 MPa (13.1 ksi)	ORNL	In progress	TN38992
700°C (1292°F)	82 MPa (11.9 ksi)	INL	In progress	BCHT-IC-9
775°C (1427°F)	45 MPa (6.5 ksi)	INL	In progress	BCHT2-IC-01
800°C (1472°F)	35 MPa (5.1 ksi)	ORNL	In progress	TN39370
300,000 hour				
600°C (1112°F)	175 MPa (25.4 ksi)	ORNL	In progress	TN39345
625°C (1157°F)	140 MPa (20.3 ksi)	ORNL	In progress	TN39368
750°C (1382°F)	45 MPa (6.5 ksi)	ORNL	In progress	TN39369
500,000 hour				
550°C (1022°F)	250 MPa (36.3 ksi)	ORNL	In progress	TN39478
575°C (1067°F)	200 MPa (29.0 ksi)	ORNL	In progress	TN39346
675°C (1247°F)	82 MPa (11.9 ksi)	ORNL	In progress	TN39344

4.2 Results

Preliminary results indicate that ESR1150AH has a significant advantage over 316H SS at the representative lifetimes of 100,000 and 300,000 hours. This advantage is less significant than the advantage NF709 has over 316H for the same lifetimes. This is shown in Figure 1(a) and Figure 1(b), which compares the rupture-stress ratio of ESR1150AH and NF709 to 316H SS as a function of temperature for a 100,000- and 300,000-hour lifetime, respectively. This analysis includes all ESR1150AH creep-rupture data collected to date. The following paragraph describes the procedure used to conduct this analysis in detail. A material can have a better, equivalent, or worse minimum rupture stress as compared to 316H SS for a given temperature and lifetime. In Figure 1, this is represented by a minimum rupture stress that is larger than one, equal to one, or less than one, respectively. The further the number deviates from one, the larger the advantage or disadvantage the material has when compared to 316H SS. For both a 100,000- and 300,000-hour lifetime, ESR1150AH has a rupture-stress ratio that is greater than 1.5, which increases with increasing temperature. For both these lifetimes, NF709 has a larger rupture-stress ratio than ESR1150AH.

These preliminary conclusions were made using a commensurable comparison of the creep strengths of these materials. The procedure to enable this comparison will now be described. First, the optimized Larson-Miller correlation was calculated, as shown in Figure 2 for: (a) ESR1150AH; (b) NF709; and (c) 316H SS. All ESR1150AH data collected to date was used when calculating this correlation. A linear Larson-Miller correlation was used for ESR1150AH and NF709. The NF709 data came from the Section I ASME BPVC Case 2581 data package to qualify NF709 seamless tubes. The 316H SS data came from the latest extended database for the alloy used by the ASME BPVC committees. Using these Larson-Miller correlations, the rupture stress for 100,000-hour and 300,000-hour lifetimes at various temperatures were predicted. The expected minimum stress-to-rupture using the ASME BPVC procedure for each material was calculated, permitting calculation of the minimum rupture-stress ratio.

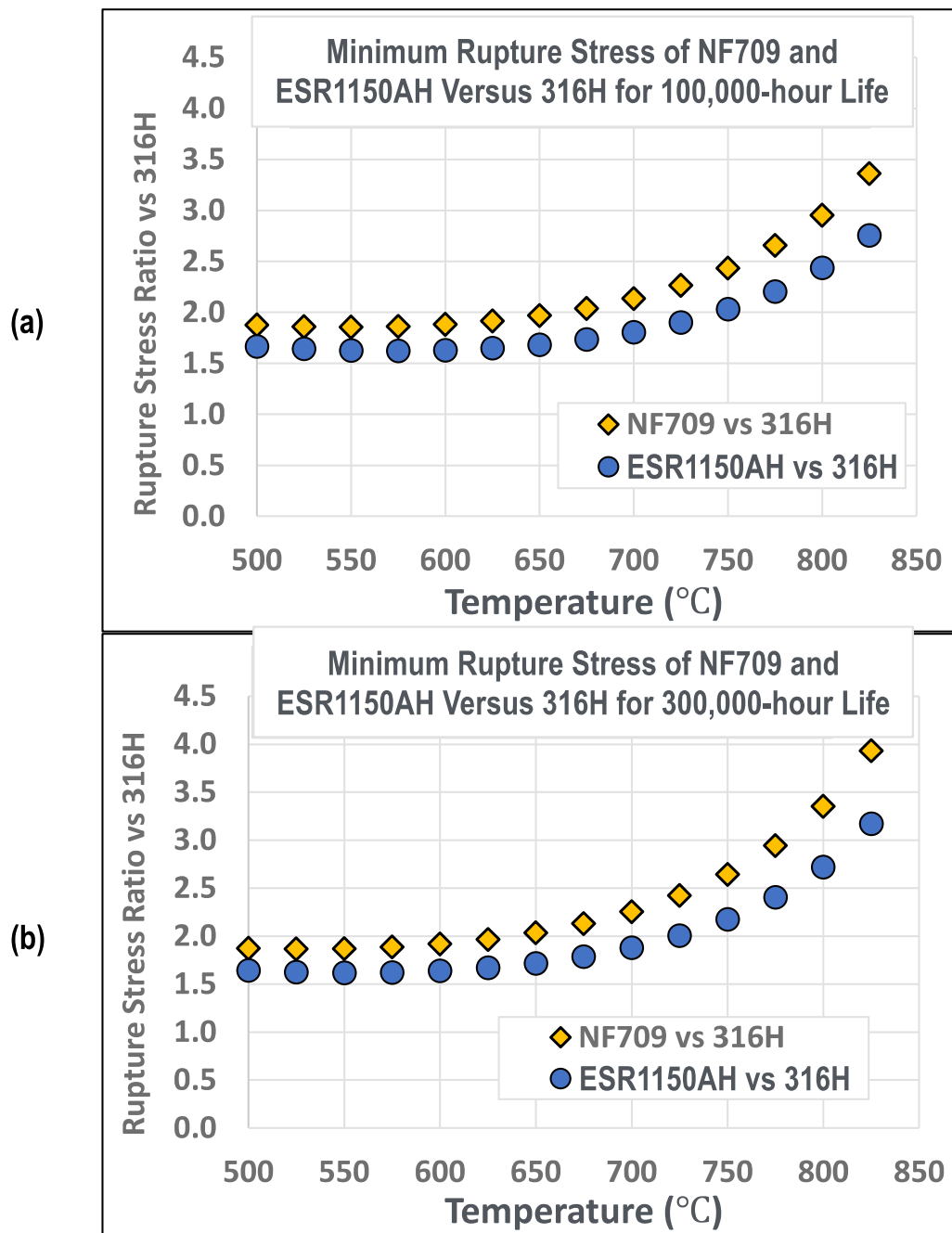


Figure 1. Rupture-stress ratio of ESR1150AH and NF709 compared to 316H SS as a function of temperature for: (a) a 100,000-hour lifetime; and (b) a 300,000-hour lifetime.

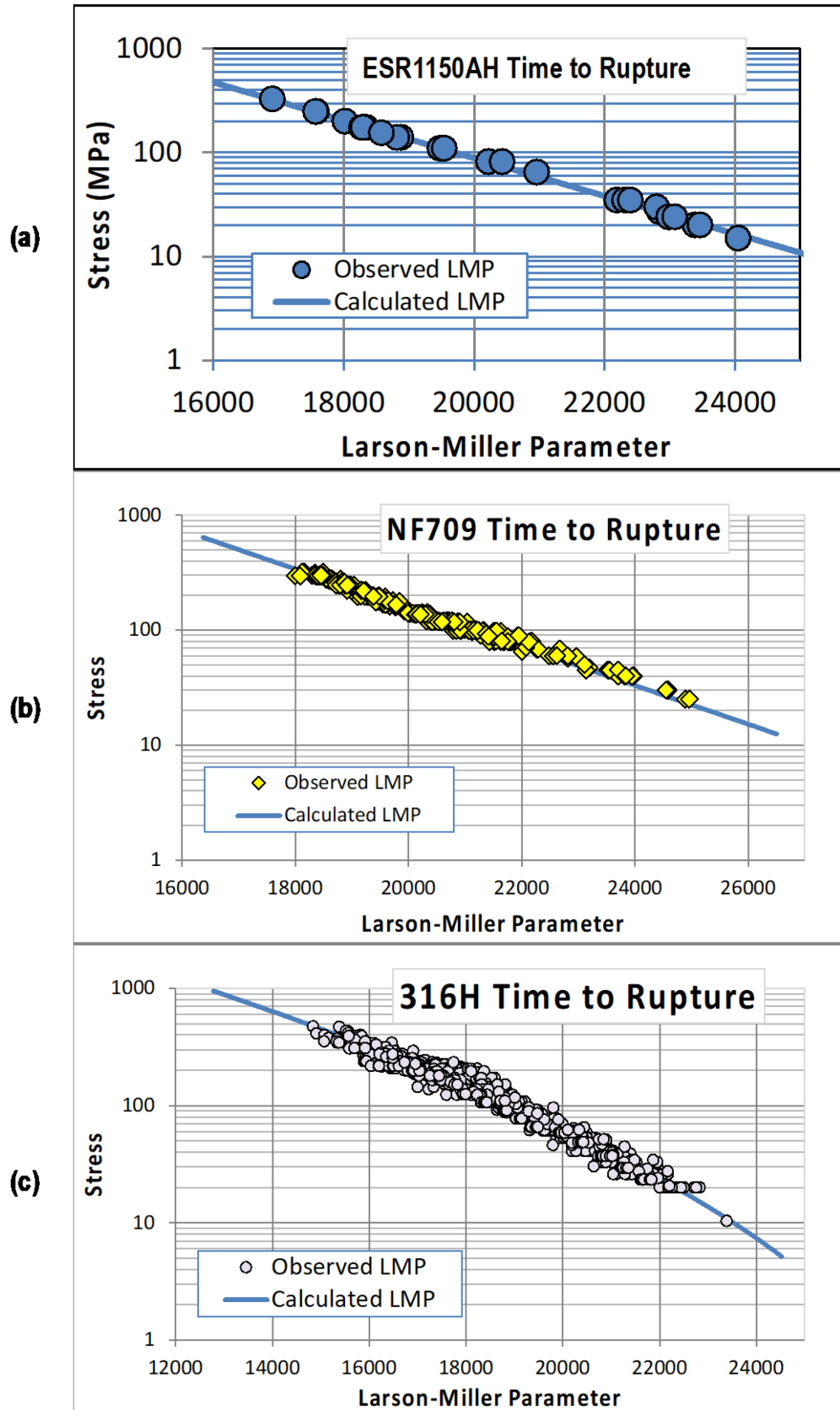


Figure 2. Optimized Larson-Miller correlation for: (a) ESR1150AH; (b) NF709; and (c) 316H SS.

NF709 having better creep-rupture properties compared to ESR1150AH is expected. NF709 was developed to optimize the creep properties for power boiler seamless tubing applications. For SFR applications, both creep strength and creep-fatigue resistance are important requiring a balance of properties. The age-hardening heat treatment was developed to accomplish this balance of properties. Even though the creep strength of ESR1150AH is reduced as compared to NF709, the advantage of ESR1150AH over 316H is still significant.

It is noted these preliminary results are exclusively from the Electralloy/G.O. Carlson heat. Additionally, tests with longer creep-rupture lives are still in progress. Creep-rupture tests from the second and third commercial heat of Alloy 709 will also be added to the Code Case testing matrix. The Larson-Miller correlation and minimum stress-to-rupture values will be updated accordingly as new test data becomes available.

5. FATIGUE CODE CASE TESTING

5.1 FY-2021 Progress

In FY-2021, a total of 12 fatigue tests were completed. Another two tests are currently in progress at the time of writing this report. These tests were conducted at INL and ORNL for the ESR1150AH processing condition. A summary of these tests is provided in Table 6.

Table 6. Fatigue tests of the ESR1150AH processing condition that transpired during FY-2021.

Temperature	Total Strain Range	Responsible Lab	Status	Sample ID
649°C (1200°F)	0.3 %	INL	In progress	BCHT-IF-5
649°C (1200°F)	0.6 %	INL	Complete	BCHT-IF-6
649°C (1200°F)	2 %	INL	Complete	BCHT-IF-7
649°C (1200°F)	3 %	INL	Complete	BCHT-IF-8
704°C (1300°F)	0.2 %	ORNL	Complete	204D_DX-33
704°C (1300°F)	0.3 %	ORNL	Complete	BCHT-OF-21_27
704°C (1300°F)	0.3 %	ORNL	Complete	BCHT_OF_19_28
704°C (1300°F)	0.6 %	ORNL	Complete	BCHT_OF_22_24
704°C (1300°F)	1 %	ORNL	Complete	BCHT_OF_14_26
816°C (1500°F)	0.25 %	INL	In progress	BCHT-IF-15
816°C (1500°F)	0.3 %	INL	Complete	BCHT-IF-14
816°C (1500°F)	0.6 %	INL	Complete	BCHT-IF-13
816°C (1500°F)	1 %	INL	Complete	BCHT-IF-12
816°C (1500°F)	3 %	INL	Complete	BCHT-IF-11

Fatigue tests were conducted in accordance with ASTM E606-12 (ASTM, 2012). Tests conducted at INL were also in accordance with PLN-3346 (Idaho National Laboratory, 2017). Testing was strain-controlled with a fully reversed ($R = -1$) triangular strain waveform with a 10^{-3} s^{-1} strain rate. Cylindrical test specimens were used with the longitudinal direction parallel to the rolling direction of the plate. Specimens were machined from the center of the plate with respect to the plate thickness. Specimens tested at INL had a 7.49 mm (0.29 in.) minimum diameter. The extensometer used at INL had a gauge length of 12 mm (0.47 in.). Specimens tested at ORNL had a 6.35 mm (0.25 in.) minimum diameter. The extensometer used at ORNL had a 12.7 mm (0.5 in.) gauge length. For a given temperature, the total strain range was selected to cover a wide range of number of cycles to failure. This enables the generation of the temperature dependent fatigue design curves. Fatigue testing up to a temperature of 816°C (1500°F) will be generated for the Alloy 709 ASME BPVC Section III, Division 5 data package. As fatigue tests finish and new data becomes available, the growing data package is continuously evaluated for gaps, and if identified, requisite tests are added to the test plan.

5.2 Results

In FY-2020, a preliminary fatigue design curve was developed at 760°C (1400°F) based on fatigue results for ESR1100 and ESR1150AH (Wang, Hou, and Sham, 2020). The results showed that the fatigue design curve of Alloy 709 was comparable to that of Alloy 800H at 760°C (1400°F). The fatigue test data collected in FY-2021 of ESR1150AH at 649°C (1200°F) were used to develop the preliminary fatigue design curves for Alloy 709 at that temperature. Additional fatigue test data at 816°C (1500°F) were collected to understand the fatigue behavior and its limits at higher temperatures. Plots of strain range versus cycles to failure are presented in Figure 3 for 649°C (1200°F) and Figure 4 for 816°C (1500°F), respectively, along with the best-fit fatigue curves. The preliminary fatigue design curve is generated using the conventional method. This entails generating two separate curves—one that is the best-fit curve with a safety factor of two applied to the strain range, and the other the best-fit curve with a safety factor of 20 applied to the number of cycles to failure. The design curve is the lesser of these two curves.

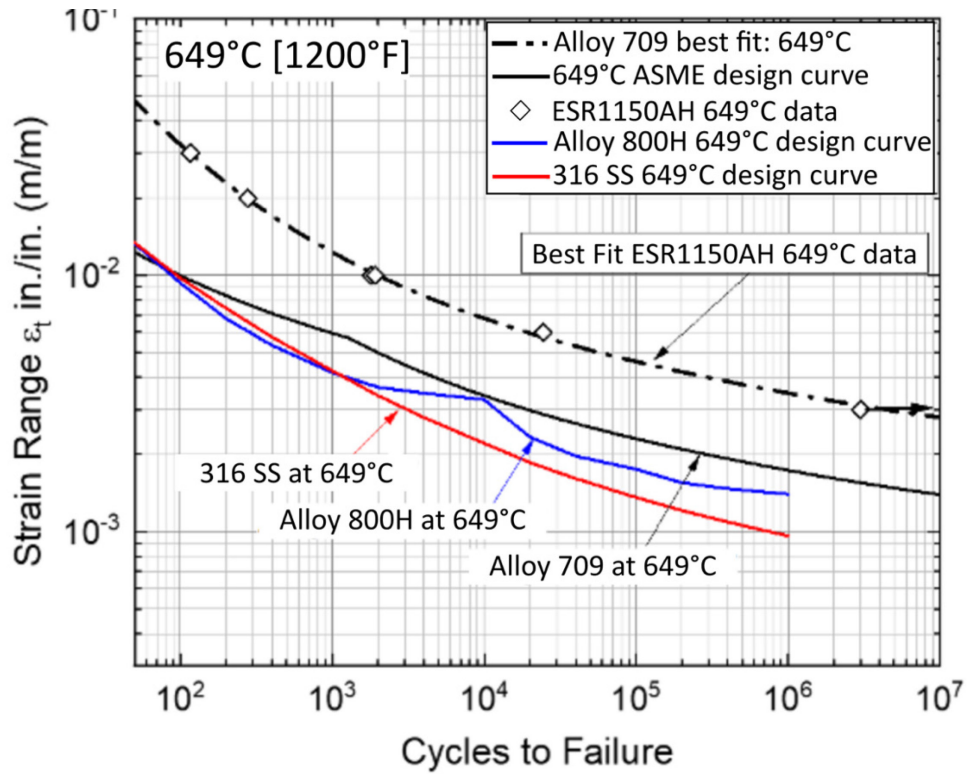


Figure 3. Preliminary fatigue design curve of Alloy 709 at 649°C (1200°F).

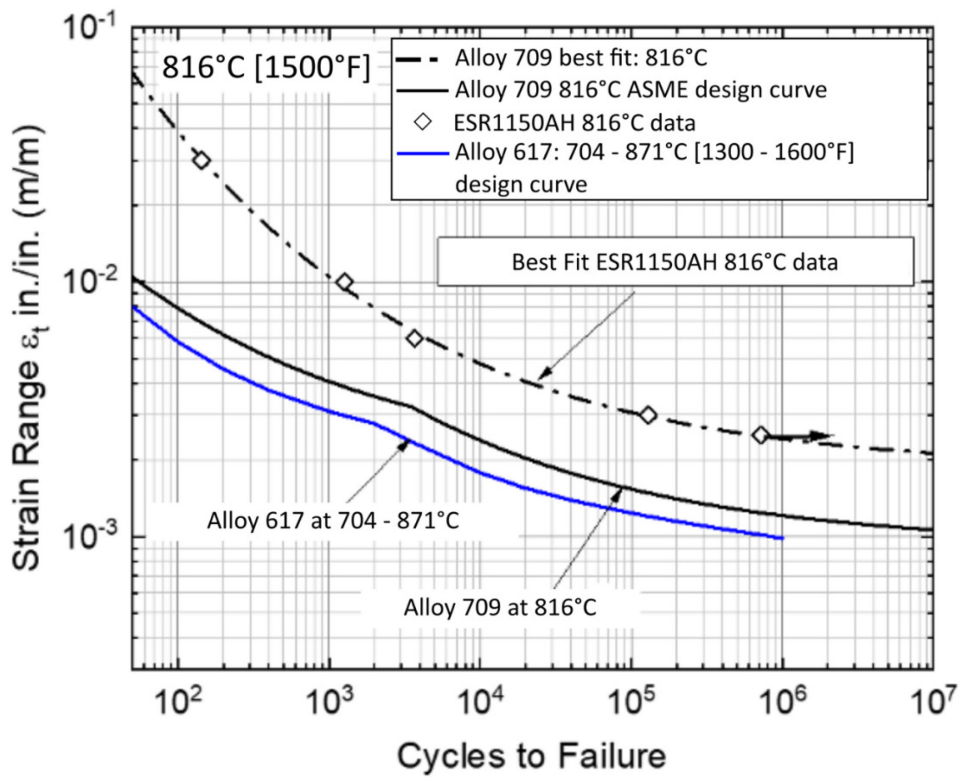


Figure 4. Preliminary fatigue design curve of Alloy 709 at 816°C (1500°F).

Alloy 709 at 649°C (1200°F) has better fatigue resistance than both Alloy 800H and 316H SS. This is shown in Figure 3 where the preliminary design curve for Alloy 709 at 649°C (1200°F) is compared with the ASME BPVC Section III, Division 5 fatigue design curves for Alloy 800H and 316H SS. The Alloy 800H fatigue design curve came from Figure HBB-T-1420-1C in Section III, Division 5 of the ASME BPVC (ASME, 2021b). The 316H SS fatigue design curve came from Figure HBB-T-1420-1B in Section III, Division 5 of the ASME BPVC. 316H SS is labeled 316 SS in Section III, Division 5 of the ASME BPVC (ASME, 2021b).

The preliminary 816°C (1500°F) fatigue design curve shown in Figure 4 was established from very limited data, five data points. Currently, although the maximum use temperature for 316H SS is 816°C (1500°F), the 316H SS fatigue design curves in Section III, Division 5, Subsection HB, Subpart B are limited to a maximum temperature of 704°C (1300°F). Alloy 800H is limited to a maximum temperature of 760°C (1400°F) (ASME, 2021b). For comparison, the ASME BPVC Case N-989 871°C (1600°F) fatigue design curve for Alloy 617 is included in Figure 4 (ASME, 2021d). This comparison shows that Alloy 709 maintains its very good fatigue performance even at higher temperatures, lending confidence to its use for temperatures up to 760°C (1400°F). Although additional fatigue data are needed to finalize the fatigue design curve at this test temperature, the preliminary results indicate the potential of extending the fatigue design curves for Alloy 709 to this temperature.

It is noted these preliminary fatigue curves were generated with data where only one specimen was tested for each test condition. All data was collected from a single heat of Alloy 709. For the Alloy 709 Code Case data package, it is expected there will be one or two replicate tests for each testing condition generated from the Electralloy/G.O. Carlson heat with the ESR1150AH processing condition. Fatigue tests from the second and third commercial heat of Alloy 709 will also be added to the Code Case testing matrix. The fatigue design curves will be updated accordingly as new test data becomes available.

6. CREEP-FATIGUE CODE CASE TESTING

6.1 FY-2021 Progress

In FY-2021, a total of 15 creep-fatigue tests were completed. These tests were conducted at INL and ORNL for the ESR1150AH processing condition. A summary of these tests is provided in Table 7.

Table 7. Creep-fatigue tests of the ESR1150AH processing condition that transpired during FY-2021.

Temperature	Nominal Total Strain Range	Hold Time	Responsible Lab	Status	Sample ID
649°C (1200°F)	0.6 %	0.167 hrs.	INL	Complete	BCHT-IF-9
649°C (1200°F)	1 %	0.167 hrs.	ORNL	Complete	BCHT_OF_3-13
649°C (1200°F)	1 %	0.5 hrs.	ORNL	Complete	BCHT_OF_8-17
649°C (1200°F)	1 %	1 hr.	ORNL	Complete	BCHT_OF_10-18
704°C (1300°F)	0.6 %	0.167 hrs.	INL	Complete	BCHT-IF-10
760°C (1400°F)	0.6 %	0.167 hrs.	ORNL	Complete	BCHT_OF_16-23
760°C (1400°F)	0.6 %	0.5 hrs.	ORNL	Complete	BCHT_OF_07-31
760°C (1400°F)	1 %	0.167 hrs.	ORNL	Complete	205D_D2-36
816°C (1500°F)	0.3 %	0.167 hrs.	ORNL	Complete	204D_D4-37
816°C (1500°F)	0.6 %	0.167 hrs.	ORNL	Complete	204D_D9-34
816°C (1500°F)	0.6 %	0.5 hrs.	ORNL	Complete	204E_E5-41
816°C (1500°F)	0.6 %	1 hr.	ORNL	Complete	204D_D6-38
816°C (1500°F)	1 %	0.167 hrs.	ORNL	Complete	204D_D7-35
816°C (1500°F)	1 %	0.5 hrs.	ORNL	Complete	204D_D3-39
816°C (1500°F)	1 %	1 hr.	ORNL	Complete	204D_D5-40

Creep-fatigue tests were conducted in accordance with ASTM E2714-13 and ASTM E606-12 (ASTM, 2013; 2012). Tests conducted at INL were also in accordance with PLN-3346 (Idaho National Laboratory, 2017). Creep-fatigue testing uses the same setup and procedures as fatigue testing. The difference between creep-fatigue and fatigue testing is the addition of a hold time to the strain waveform at the maximum tensile strain. Test conditions were selected to cover a spectrum of temperatures, total strain ranges, and hold times. This is necessary to establish the creep-fatigue damage envelope. As creep-fatigue tests finish and new data become available, the growing data package is continuously evaluated for gaps, and if identified, requisite tests are added to the test plan.

6.2 Results

The damage envelope in the D-diagram for Alloy 709 may have its interaction point at (0.2, 0.2). This was inferred from Figure 5, which includes all available ESR1150AH data on the D-diagram. The data points in Figure 5 are color coded based on the temperature that the creep-fatigue test was conducted at. Possible interaction points of (0.2, 0.2), (0.3, 0.3), and (0.4, 0.4) and the corresponding bilinear curves are included in Figure 5 as well. The bilinear curves show possible damage envelopes. Creep-fatigue data from more test conditions and other commercial heats are required before a definitive intersection point can be determined. For the Alloy 709 Code Case data package, more creep-fatigue data will be collected from the Electralloy/G.O. Carlson heat as well as the second and third commercial heat of Alloy 709. The D-diagram as well as the damage envelope will be updated as new test data becomes available.

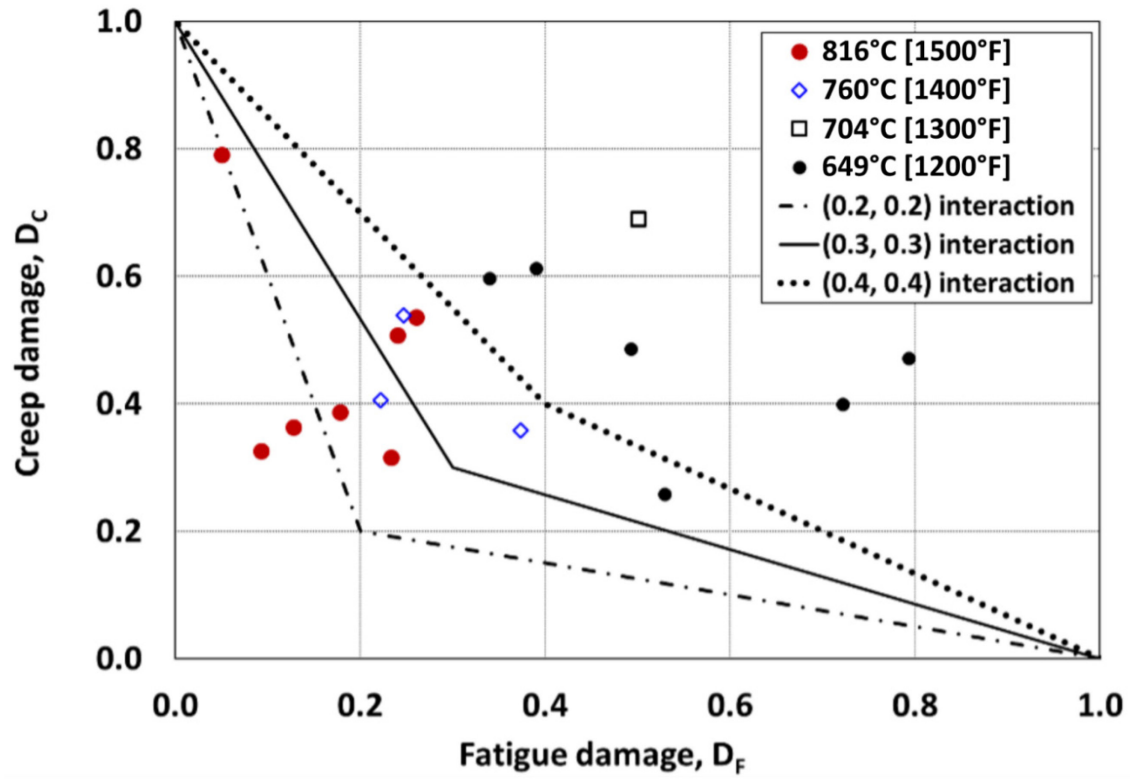


Figure 5. Preliminary creep-fatigue D-diagram for Alloy 709.

7. SUMMARY AND ONGOING WORK

Alloy 709 is an advanced material that offers many advantages over 316H SS and would improve the viability of SFRs. Consequently, it has been identified as the next alloy to be qualified in Section III, Division 5 of the ASME BPVC. The Alloy 709 Code Case data package is currently being developed through a collaboration between ANL, INL, and ORNL. An update is provided on the status of creep, fatigue, and creep-fatigue testing that transpired during FY-2021 at ANL, INL, and ORNL. Preliminary results continue to demonstrate the improved creep and fatigue resistance of Alloy 709 compared to 316H SS.

In FY-2020, INL placed a purchase order with Allegheny Technologies Incorporated (ATI) to procure the second commercial heat of Alloy 709 (Wright, 2020). The Alloy 709 plates, heat 529900, were delivered by ATI in March 2021. This heat is in the process of being characterized to determine its quality. Once the quality is deemed to be satisfactory, Code Case testing of this plate will commence. This includes creep, fatigue, and creep-fatigue testing. This testing will be in conjunction with the creep and fatigue tests that are currently in progress at the time of writing this report as well as the planned tests for the Electralloy/ G.O. Carlson heat discussed in this report. Finally, procurement of the third commercial heat of Alloy 709 is currently in progress. The material is expected to be received at INL next fiscal year.

8. REFERENCES

- ASME International. 2021a. "Section II, Part D, M: Materials, Properties (Metric)." In *ASME Boiler and Pressure Vessel Code: An International Code*. New York, NY: ASME.
- ASME International. 2021b. "Section III, Division 5: Rules for Construction of Nuclear Facility Components, High Temperature Reactors." In *ASME Boiler and Pressure Vessel Code: An International Code*. New York, NY: ASME.
- ASME International. 2021c. "Standard Specification for Seamless Ferritic and Austenitic Alloy-Steel Boiler, Superheater, and Heat Exchanger Tubes." ASME SA-213/SA-213M. New York, NY.
- ASME International. 2021d. "Use of Alloy 617 (UNS N06617) for Class A Elevated-Temperature Service Construction: Section III, Division 5." Case N-898. New York, NY.
- ASME International. 2021e. "20Cr-25Ni-1.5Mo-Cb-N Seamless Austenitic Stainless Steel Tube, Section I." Case 2581. New York, NY.
- ASTM International. 2011. "Standard Test Methods for Conducting Creep, Creep-Rupture, and Stress-Rupture Tests of Metallic Materials." ASTM E139-06. West Conshohocken, PA.
- ASTM International. 2012. "Standard Test Method for Strain-Controlled Fatigue Testing." ASTM E606/E606M-12. West Conshohocken, PA.
- ASTM International. 2013. "Standard Test Method for Creep-Fatigue Testing." ASTM E2714-13. West Conshohocken, PA.
- ASTM International. 2021. "Standard Specification for Seamless Ferritic and Austenitic Alloy-Steel Boiler, Superheater, and Heat-Exchanger Tubes." ASTM A213/A213M-21a. West Conshohocken, PA.
- Executive Order No. 14,008. 2021. 3 C.F.R 7624. "Tackling the Climate Crisis at Home and Abroad." January 27, 2021.
- Idaho National Laboratory. 2016. "Creep Testing." PLN-3386 INL/MIS-16-40783-Rev002, Idaho National Laboratory.
- Idaho National Laboratory. 2017. "Creep Fatigue Testing." PLN-3346 INL/MIS-10-18953-Rev009, Idaho National Laboratory.
- Larson, F.B., and James Miller. 1952. "A Time-Temperature Relationship for Rupture and Creep Stresses." *Transactions of the ASME* 74: 765-771.
- McMurtrey, Michael. 2018. "Report on the FY-2018 Creep Rupture and Creep-Fatigue Tests on the First Commercial Heat of Alloy 709." INL/EXT-18-46140-Rev000, Idaho National Laboratory. <https://doi.org/10.2172/1484686>.
- McMurtrey, Michael and Ryann Rupp. 2019. "Report on FY-2019 Scoping Creep and Creep-Fatigue Testing on Heat Treated Alloy 709 Base Metal." INL/EXT-19-55502-Rev000, Idaho National Laboratory.
- Natesan, Krishnamurti, Xuan Zhang, Ting-Leung Sham, and Hong Wang. 2017. "Report on the Completion of the Procurement of the First Heat of Alloy 709." ANL-ART-89, Argonne National Laboratory. <https://doi.org/10.2172/1364649>.
- Natesan, Krishnamurti, Xuan Zhang, and Meimei Li. 2018. "Report on the initiation of planned FY18 short and intermediate term creep rupture tests and creep-fatigue tests on the first commercial heat of Alloy 709." ANL-ART-51, Argonne National Laboratory. <https://doi.org/10.2172/1485134>.

- O'Donnell, William J., and Donald S. Griffin. 2007. "Regulatory Safety Issues in the Structural Design Criteria of ASME Section III Subsection NH and for Very High Temperatures for VHTR & GEN IV." DOE/ID14712-2, ASME Standards Technology, LLC. <https://doi.org/10.2172/974279>.
- Rupp, Ryann E., and Michael D. McMurtrey. 2020. "Mechanical Properties of Aged A709." INL/EXT-20-59630-Rev000, Idaho National Laboratory.
- Sham, Ting-Leung and Krishnamurti Natesan. 2017. "Code Qualification Plan for an Advanced Austenitic Stainless Steel, Alloy 709, for Sodium Fast Reactor Structural Applications." International Conference on Fast Reactors and Related Fuel Cycles: Next Generation Nuclear for Sustainable Development (FR17), Yekaterinburg, Russia, IAEA-CN-245-74.
- Swindeman, Robert W., Michael J. Swindeman, Blaine W. Roberts, Brian E. Thurgood, and Douglas L. Marriott. 2007. "A Review of Available Tensile and Creep-Rupture Data Sources and Data Analysis Procedures for Deposited Weld Metal and Weldments of Alloy 800H."
- Thomas, Brian E. 2018. "NRC Response to ASME Letter of Request for NRC Endorsement of ASME Boiler and Pressure Vessel Code, Section III, Division 5". ML18211A571, United States Nuclear Regulatory Commission.
- Wang, Hong, C. Shane Hawkins, Eric C. Disney, and Jeremy L. Moser. 2018. "The Initiation of Long-Term Creep Rupture Tests on the First Alloy 709 Commercial Heat." ORNL/TM-2018/985, Oak Ridge National Laboratory. <https://doi.org/10.2172/1476397>.
- Wang, Yanli and Ting-Leung Sham. 2019. "Planned FY-2019 Creep and Fatigue Design Curve Testing of Alloy 709 Base Metal." ORNL/TM-2019/1303, Oak Ridge National Laboratory. <https://doi.org/10.2172/1569365>.
- Wang, Yanli, Peijun Hou, and Ting-Leung Sham. 2020. "Report on FY-2020 Creep, Fatigue, and Creep-Fatigue Testing of Alloy 709 Base Metal at ORNL." ORNL/TM-2020/1622, Oak Ridge National Laboratory. <https://doi.org/10.2172/1671410>.
- Wang, Yanli, Peijun Hou, and Ting-Leung Sham. 2021. "Report on FY-2021 Creep, Fatigue, and Creep Fatigue Testing of Alloy 709 Base Metal at ORNL." ORNL/TM-2021/2120, Oak Ridge National Laboratory.
- Wright, Jill K., Laura J. Carroll, Ting-Leung Sham, Nancy J. Lybeck, and Richard N. Wright. 2016. "Determination of the Creep-Fatigue Interaction Diagram for Alloy 617." Proceedings of the ASME 2016 Pressure Vessels and Piping Conference, Vancouver, British Columbia, Canada, PVP2016-63704.
- Wright, Richard N. 2020. "Report Documenting Activity for Second Alloy 709 Commercial Heat." INL/EXT-20-59880-Rev000, Idaho National Laboratory.
- Zhang, Xuan, and Ting-Leung Sham. 2019. "FY-2019 Status Report on Creep Test Data on Commercial Heat of Alloy 709." ANL-ART-172, Argonne National Laboratory. <https://doi.org/10.2172/1601809>.
- Zhang, Xuan, Ting-Leung Sham, and George A. Young. 2019. "Microstructural Characterization of Alloy 709 Plate Materials with Additional Heat Treatment Protocol." ANL-ART-170, Argonne National Laboratory. <https://doi.org/10.2172/1601459>.
- Zhang, Xuan, and Ting-Leung Sham. 2020. "FY-2020 Status Report on Creep Rupture Testing to Support the Development of Alloy 709 Code Case." ANL-ART-193, Argonne National Laboratory. <https://doi.org/10.2172/1656611>.
- Zhang, Xuan, Ting-Leung Sham, and Meimei Li. 2021. "FY-2021 Status Report on Creep Rupture Testing at ANL to Support the Development of Alloy 709 Code Case." ANL-ART-231, Argonne National Laboratory. <https://doi.org/10.2172/1810715>.